Conservative Analytical Collision Probability for Design of Orbital Formations

J. Russell Carpenter*

NASA Goddard Space Flight Center

The literature offers a number of approximations for analytically and/or efficiently computing the probability of collision between two space objects. However, only one of these techniques is a completely analytical approximation that is suitable for use in the preliminary design phase, when it is more important to quickly analyze a large segment of the trade space than it is to precisely compute collision probabilities. Unfortunately, among the types of formations that one might consider, some combine a range of conditions for which this analytical method is less suitable. This work proposes a simple, conservative approximation that produces reasonable upper bounds on the collision probability in such conditions. Although its estimates are much too conservative under other conditions, such conditions are typically well suited for use of the existing method.

Notation

Description	Example	Represents
Lower case italic type	a	scalars
Upper case italic type	A	matrices
Bold type (either case)	$\mathbf{r}$	vectors

I. Introduction

One of the new challenges of flying close formations of spacecraft over mission durations of months to years is to maintain adequate collision avoidance margins. In general, computation of collision probability requires quadrature, which can be cumbersome for conceptual design and trade studies. A number of approximations have appeared in the literature, some of which the sequel will describe, that offer a wide range of trade-offs between accuracy or conservatism, applicability to the formation flying problem, and computational complexity and efficiency.

In the design phase, it is important to understand the relationship between collision avoidance objectives and navigation system capabilities. Especially in the early conceptual design phase, accuracy is less important than insight. In such an early phase of design, one needs the ability to implement simple equations in a spreadsheet so as to examine large wedges of the trade space. One can accept coarse approximations, so long as these approximations are not too lacking or abundent in conservatism. To this end, after reviewing and discussing the literature, this paper proposes a conservative approximation for collision probability. A designer might use this approximation in the process of conceptually studying the flight dynamics issues for an orbital formation flying mission.

*Flight Dynamics Analysis Branch, Code 595, Greenbelt, MD 20771.   Fax: 301-286-7526.   Email: Russell.Carpenter@nasa.gov.

II. Problem Description

The relative position and velocity between two satellites are

$$\mathbf{r} = \mathbf{R}_2 - \mathbf{R}_1 \tag{1}$$

$$\mathbf{v} = \mathbf{V}_2 - \mathbf{V}_1 \tag{2}$$

$$\mathbf{v}_{rel} \equiv \mathbf{v} - \boldsymbol{\omega}_1 \times \mathbf{r} \tag{3}$$

where $\boldsymbol{\omega}_1$ is the instantaneous orbital angular velocity of spacecraft 1. The relative position is uncertain due to navigation errors, $\mathbf{e}$,

$$\mathbf{r} = \bar{\mathbf{r}} + \mathbf{e} \tag{4}$$

where $\bar{\mathbf{r}} = \mathrm{E}\,[\mathbf{r}]$ is the nominal relative position vector. The associated covariance matrix, in whatever coordinates the quantities of Eq. 1 are specified, is

$$P = \mathrm{E}\left[(\mathbf{r} - \bar{\mathbf{r}})(\mathbf{r} - \bar{\mathbf{r}})^{\mathrm{T}}\right] \tag{5}$$

$$= P_{R1} + P_{R2} - P_{R1R2} - P_{R1R2}^{\mathrm{T}} \tag{6}$$

where

$$P_{Ri} = \mathrm{E}\left[(\mathbf{R}_i - \mathrm{E}\,[\mathbf{R}_i])(\mathbf{R}_i - \mathrm{E}\,[\mathbf{R}_i])^{\mathrm{T}}\right] \tag{7}$$

$$P_{RiRj} = \mathrm{E}\left[(\mathbf{R}_i - \mathrm{E}\,[\mathbf{R}_i])(\mathbf{R}_j - \mathrm{E}\,[\mathbf{R}_j])^{\mathrm{T}}\right] \tag{8}$$

Note that the equations above only consider position errors. Note also that the cross-covariance matrix P_{RiRj} and its transpose often contain significant correlations for the formation flying problem, since intersatellite measurements such as cross-link ranges may be used in the navigation filter.

Figure 1 illustrates the problem geometry. The figure depicts two local coordinate frames that are fixed to planes: the tangent plane and the conjunction plane. The former is tangent to the nominal trajectory of spacecraft 1, and has its corresponding basis vectors defined as follows,

$$\tilde{\mathbf{t}}_1 = \frac{\mathbf{V}_1}{\|\mathbf{V}_1\|} \tag{9}$$

$$\tilde{\mathbf{t}}_2 = \frac{\mathbf{R}_1 \times \mathbf{V}_1}{\|\mathbf{R}_1 \times \mathbf{V}_1\|} \tag{10}$$

$$\tilde{\mathbf{t}}_3 = \tilde{\mathbf{t}}_1 \times \tilde{\mathbf{t}}_2 \tag{11}$$

The conjunction frame contains the relative position vector, with basis vectors defined as

$$\tilde{\mathbf{c}}_1 = \frac{\bar{\mathbf{r}}}{\|\bar{\mathbf{r}}\|} \tag{12}$$

$$\tilde{\mathbf{c}}_2 = \tilde{\mathbf{c}}_3 \times \tilde{\mathbf{c}}_1 \tag{13}$$

$$\tilde{\mathbf{c}}_3 = \frac{\bar{\mathbf{r}} \times \bar{\mathbf{v}}_{rel}}{\|\bar{\mathbf{r}} \times \bar{\mathbf{v}}_{rel}\|} \tag{14}$$

Due to the navigation errors, the point at which the path of spacecraft 2 relative to spacecraft 1 penetrates the conjunction plane is uncertain, which Figure 1 illustrates by associating color warmth with probability of penetration. The conjunction plane generally cuts an oblique cross-section of the three-dimensional error ellipsoid associated with the navigation errors, as Figure 2 shows.
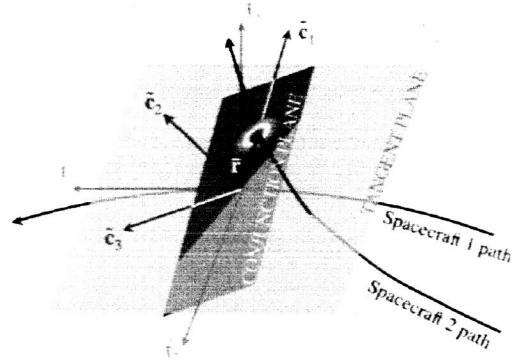

Figure 1. Conjunction geometry. Warmer colors indicate regions of conjunction plane with higher probabilities of penetration. Spacecraft paths represent nominal trajectories.
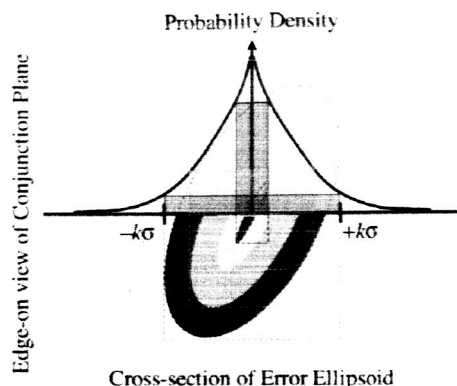
Figure 2. Edge-on view of conjunction plane. In upper half of figure, height above plane indicates probability density in the plane of conjunction. Lower half of figure depicts cross-section of 3-dimensional error ellipsoid, which is repeated in outline form in upper half.

The goal of collision avoidance is to ensure that the actual relative position vector remains outside some collision avoidance region, which in this work is taken as a sphere of radius a, as Figure 3 depicts. A corresponding collision avoidance requirement would be

$$\Pr\{\|\mathbf{r}\| \geq a\} \geq 1 - \epsilon, \tag{15}$$

where ϵ is as small as practicable.

The problem just defined is quite similar to the problem of calculating the probability for a single spacecraft to avoid a piece of space debris. The primary differences are as follows. In debris encounters, the relative orbits between the spacecraft and the debris are generally quite different, so that very brief and infrequent conjuctions between them occur. In these encounters, the relative velocity is typically quite high, and the relative motion is essentially rectilinear over the brief period near closest approach. It is also generally true that the uncertainty associated with the debris orbits is quite large in comparison with the combined cross-sectional area of the spacecraft and the debris, and that little or no cross-correlation exists between the estimated states of the spacecraft and the debris. In most formations and many constellations, none of these conditions is likely to be satisfied.

III. Background

Foster and Estes[1] show that under certain conditions typical of most debris encounters, only the projection of the three-dimensional error ellipsoid onto the conjunction plane at the point of closest approach need be considered when computing the probability of collision. Akella and Alfriend[2] show the equivalence between integration over the conjunction plane and integration over the full three-dimensional ellipsoid, under these conditions. The upper half of Figure 2 represents a section of this two-dimensional density as height above the conjunction plane, and the color mapping of the conjunction plane in Figures 1 and 3 represents contours of equal probability in this two-dimensional density. Thus, to determine the probability of collision, one need only find the cumulative density above the collision avoidance region, i.e. the volume bounded above by the density function, and along its periphery by the collision avoidance boundary. This integral in general requires quadrature. A number of approximate alternatives to quadrature have appeared in the literature, among which Patera[3] describes a reduction
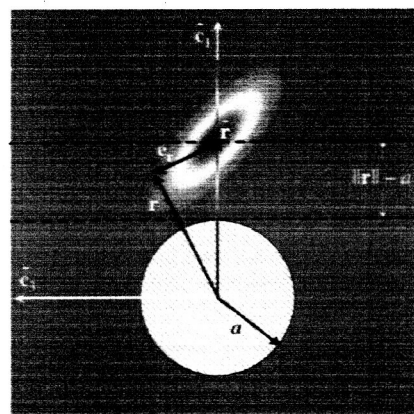

Figure 3. Collision avoidance geometry. Cross-hatching indicates the region to be protected. The higher-probability-of-penetration region should not intersect the avoidance region.

of the two-dimensional integral to a numerical line integral, that can adequately describe the probability for complex avoidance regions, so long as the region of uncertainty is symmetric.

Chan[4] describes an approximate alternative to quadrature that is completely analytical, and therefore a good candidate for the type of algorithm sought in this work. This approach is based on an approximate transformation of the debris avoidance problem to the problem of computing the probability that a realization of a symmetric, two-dimensional random variable lies within a circular disk, when the mean of the random variable does not coincide with the center of the disk. This is an example problem in the 1965 edition of

Papoulis,[5] and the resulting density contains a modified Bessel function. Chan expresses the density in series form, integrates term by term to find an approximation of the probability, shows that in most cases typical of debris avoidance, retaining only the first term is adequate, and finally gives error bounds on each truncation of the series. Since in most realistic problems, the covariance is not isotropic, i.e. its error ellipsoids are not spheres, Chan introduces a second approximation. If the avoidance region is circular, a coordinate system rotation to the covariance's principal axes will at least remove the complexity introduced by any correlations. However, the method of integration used in Papoulis' example relied on the circular symmetry of the isotropic density. A common technique of introducing a non-isotropic dilation of coordinates to circularize the covariance will not work in this case, since this will make the circular avoidance region into an ellipse. Chan addresses this problem by simply substituting a circular avoidance region that has the same area as the ellipse representing the actual avoidance region, in the dilated coordinates. Reference 4 documents agreement to within two or three significant digits between this method and several other numerical alternatives, for certain conditions typical of many debris encounters. However, the author notes that "it is possible to assign values to these parameters such that this model yields poor approximations," and in particular suggests that whenever either the size of the avoidance region or the nominal miss distance is of the same order as the standard deviation of the isotropic density, the method will fail. Chan suggests breaking up the cross-section in order to address this shortcoming, but does not describe how one should do this.
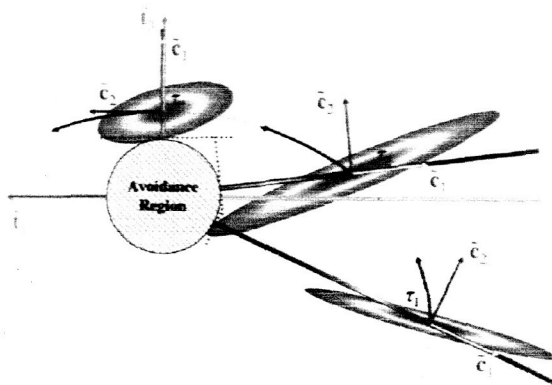

Figure 4. Relative motion during a portion of one orbit for a formation or constellation. The variable τ represents a non-decreasing index, such as time or true anomaly, and τ_* represents its value at the time of closest approach.

Unfortunately, the conditions under which the volume integral may be reduced to an area integral in the conjuction plane are not typical of most close encounters between spacecraft in a constellation or formation. Most importantly, the relative velocity is generally much lower, so that the time the spacecraft spend within close proximity to one another is significant. As a result, one may not ignore the time-varying nature of the relative motion and the relative error covariance, as Figure 4 illustrates.

Peterson[6] suggests that anytime the velocity uncertainty approaches the magnitude of the relative velocity itself, the velocity uncertainty should not be ignored. For such "long-term encounter" cases, Chan[7] proposes an extension of Reference 4. In this work, after a series of scale transformations and rotations, the avoidance region becomes an ellipsoid rotating about an isotropic covariance, contained with a three-dimensional tangent hypersurface that corresponds to a toroid for many relevant circumstances. In such cases, the boundaries of the relative motion in the transformed coordinates may be approximated by ellipses, but in order to make use of the approximate analytical technique of Reference 4, Chan approximates the boundaries instead with circles.

Chan[8] and Campbell[9] directly address the case of formation flying to varying degrees. Reference 8 couples the previously published techniques of References 4 and 7 for collision assessment with a new method for performing collision avoidance maneuvers that minimizes the collision probability. Reference 9 considers that the error distributions may become non-Gaussian through the action of the nonlinear relative motion dynamics, as Junkins, et al.[10] and Lee and Alfriend[11] demonstrate, and proposes a solution involving ellipsoidal bounds for the distributions. Campbell then compares two analytical methods that use these bounding ellipsoids to conservatively approximate the collision probability, and compares these to a numerical solution. The first technique is an approximate solution to the non-trivial problem of maintaining an estimate of the minimum distance between ellipsoids of constant probability mass for each satellite, as the relative trajectories evolve in time, and gives the more conservative estimate for the collision probability. If the ellipsoids do not overlap, then the estimate of the collision probability is bounded by the probability mass that is not contained within the ellipsoids. If the ellipsoids do overlap, then Campbell's method transitions to a second more accurate approximation. The second method is based on finding the ellipsoid that bounds the intersection, and using this to perform a refinement of the first technique using a discrete set of error

ellipsoids that contain varying probability masses, to find the largest collision probability that does not result from an intersection.

IV. Approximate Solution

Suppose that one does not care to compute the actual probability of collision, but instead would be satisfied with a lower bound on the probability of *not* having a collision, which would then imply a conservative upper bound on the probability of collision. Suppose further that this bound on the collision probability were to primarily be used during the conceptual design phase of a formation flying mission, to get a sense of trades among such factors as relative navigation accuracy, sizes of control boxes, etc., rather than for use during detailed design or operations. Under such circumstances, one could tolerate a fairly conservative bound on the collision probability, and in fact such conservatism would likely be desirable. This section will show that one may obtain such a bound by merely finding the marginal probability of collision along the relative position vector. However, it may be helpful to describe the approach first.

Referring to Figures 3 and 4, imagine dividing the space containing the avoidance region, and some specified, central portion of the error distribution, by a surface separating these two regions. If the relative trajectory contains loops or cusps, this surface may be quite topologically complex. Unlike the closed surfaces decribed in Reference 7, the surface this work imagines need only divide the space into two regions, one containing a specified portion of the probability mass and the other containing the avoidance region. The dotted lines in Figure 4 indicate cross-sections of planes tangent to such a surface. At any given point in time, the normal of such a tangent plane is the relative position vector. Now, at any instant, the probability mass that is further from the avoidance region than the nominal relative position, can only decrease the probability of collision at that instant, so one need not consider it at that instant. Therefore, since the nominal relative position is the center of the error distribution, one need only consider the half of its mass that is closer to the avoidance region. Within this half, the region between the nominal relative position and the plane tangent to the avoidance region, and centered along the axis of the relative position, will contain any tails of the distribution that extend toward the avoidance region. It is only the probability mass that extends beyond this region that contributes to collision probability at any particular instant. Integration over this region results in the marginal probability along the relative position. Clearly, the vast majority of this mass does not overlap the avoidance region, making this approach a coarse estimate of the collision probability. However, if one views Figures 3 and 4 as typical of the desired trajectory of a formation flying mission, i.e. the size of the avoidance region is of the same order as the uncertainty of the relative position, and the separation between these is of at least this order, then very little mass exists in this region, and including it in the probability of collision will not contribute much to overestimating the collision probability. Situations such as these are exactly the ones that the method of Reference 4 fails to handle. In the converse situation, Reference 4 provides a highly accurate and efficient technique.

Before describing the coarse method further, since the definition of the error function is not always consistent, note that in this work, its definition is

$$\text{erf}(k) = \frac{1}{\sqrt{2\pi}\sigma} \int_{-k\sigma}^{+k\sigma} e^{-\frac{1}{2}\frac{x^2}{\sigma^2}} \, dx \tag{16}$$

To compute this integral in *Matlab*, use `erf(k/sqrt(2))`; to compute it in *Excel*, use `NORMDISTS(k) - NORMDISTS(-k)`. Next, let

$$C(\tau) = \begin{bmatrix} \tilde{\mathbf{c}}_1(\tau) & \tilde{\mathbf{c}}_2(\tau) & \tilde{\mathbf{c}}_3(\tau) \end{bmatrix}; \tag{17}$$

and let u, v, and w represent coordinates along the $\tilde{\mathbf{c}}_1$, $\tilde{\mathbf{c}}_2$, and $\tilde{\mathbf{c}}_3$ axes, respectively; then, the relative position error and its covariance projected onto the conjunction coordinates are $\mathbf{e}_c(\tau) = C^T(\tau)\mathbf{e}(\tau)$ and

$$P_c(\tau) = C^T(\tau)P(\tau)C(\tau) = \begin{bmatrix} \sigma_u^2 & \rho_{uv}\sigma_u\sigma_v & \rho_{uw}\sigma_u\sigma_w \\ \cdot & \sigma_v^2 & \rho_{vw}\sigma_v\sigma_w \\ \cdot & \cdot & \sigma_w^2 \end{bmatrix} \tag{18}$$

The density function of the conjunction frame errors, assuming a Gaussian distribution is,[12]

$$f_{uvw}(u,v,w;\tau) = \frac{1}{\sqrt{(2\pi)^3|P_c(\tau)|}} e^{-\frac{1}{2}\mathbf{e}_c(\tau)^T P_c^{-1}(\tau)\mathbf{e}_c(\tau)} \tag{19}$$

From Figures 3 and 4, the total probability mass "in-between" the nominal relative position and the edge of the avoidance region is

$$p_i = \int_{-\infty}^{\infty} \int_{-\infty}^{\infty} \int_{\|\bar{\mathbf{r}}\|-a}^{\|\bar{\mathbf{r}}\|} f_{uvw}(u,v,w;\tau) du\, dv\, dw;$$

note that

$$\int_{-\infty}^{\infty} \int_{-\infty}^{\infty} f_{uvw}(u,v,w;t) dv\, dw = \frac{1}{\sqrt{2\pi}\sigma_u(\tau)} e^{-\frac{1}{2}\frac{u^2}{\sigma_u^2}} = f_u(u;\tau) \tag{20}$$

is just the marginal density over u, which is the projection of the density onto the $\tilde{\mathbf{c}}_1$ axis, as the shading of this axis in Figures 3 and 4 indicate. As a result, the total "in-between" probability mass is

$$\int_{\|\bar{\mathbf{r}}\|-a}^{\|\bar{\mathbf{r}}\|} f_u(u;\tau) = \int_{-k\sigma_u}^{0} \frac{1}{\sqrt{2\pi}\sigma_u} e^{-\frac{1}{2}(u')^2/\sigma_u^2} du'$$
$$p_i = \frac{1}{2}\mathrm{erf}(k) \tag{21}$$

where u' is along $\tilde{\mathbf{c}}_1$ and has as its origin the center of the distribution, and

$$k = (\|\bar{\mathbf{r}}\| - a)/\sigma_u. \tag{22}$$

Dropping the prime notation, it is clear from the symmetry of the Gaussian distribution that

$$\int_{-k\sigma_u}^{0} f_u(u;\tau) du = \frac{1}{2} - \int_{-\infty}^{-k\sigma_u} f_u(u;\tau) du \tag{23}$$

and

$$\int_{-\infty}^{-k\sigma_u} f_u(u;\tau) du > \int_{-\|\bar{\mathbf{r}}\|-a}^{-\|\bar{\mathbf{r}}\|+a} f_u(u;\tau). \tag{24}$$

Also, the true probability of collision, p_c, is bounded by

$$p_c < \int_{-\|\bar{\mathbf{r}}\|-a}^{-\|\bar{\mathbf{r}}\|+a} f_u(u;\tau). \tag{25}$$

Therefore, backtracking through Eqs. 25, 24, 23, and 21, the coarse bound is finally

$$p_c < \frac{1}{2} - \frac{1}{2}\mathrm{erf}(k). \tag{26}$$
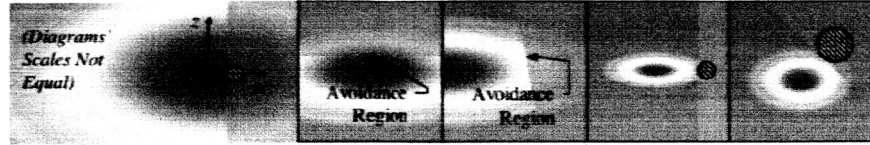
The sequel provides examples of how the coarse bound compares with Chan's method, and of how to use Eq. 21 in the preliminary design of a formation flying mission.

V.   Examples

Table 1 illustrates several two-dimensional scenarios, and compares the coarse method with the method of Reference 4. The first two columns are taken from Reference 4. Clearly, the coarse method is far too conservative for the cases in which Chan's method works well, which the first three columns illustrate. This is most clear in the example that the first column describes. Here the shaded region, over which the coarse method integrates, covers nearly half of the highest density portions of the distribution, while the actual avoidance region, although it is in a high density region, is quite small. Similar though less drastic inclusions of extra density occur in the examples that columns two and three describe. However, as the last two columns show, the coarse appears to produce quite reasonable bounds on the collision probability for cases that may be more typical for formations, in which a relatively larger avoidance area is nominally going to be kept well outside the higher density portions of the relative error distribution. Note also that the error bounds on Chan's method indicate that it is not producing reliable approximations in these cases.

The coarse method also produces less conservative and more accurate bounds whenever the avoidance region covers a significant portion of the higher density portions of the error distribution. For example, if one increases the size of the avoidance region in column one of Table 1 to the order of the standard deviation,

Table 1. Examples comparing several scenarios. The gray-shaded region is the area over which the coarse method integrates. The red-shaded region approximates the 1σ density envelope. The directions x and z are along the major and minor axes of the density in the conjuction plane. The rows labeled "Chan" use the methods of Reference 4, and include bounds which are a good indicator as to when that method fails.

(Diagrams Scales Not Equal)					
σ_x [m]	50	3000	3000	100	100
σ_z [m]	25	1000	1000	20	50
a [m]	5	10	50	50	100
x [m]	10	0	5000	300	200
z [m]	0	1000	1000	0	200
p_c [Chan, 1-term]	9.753e-3	1.011e-5	6.542e-5	0.005	3e-5
p_c [Chan 1-term upper bound]	9.755e-3	1.011e-5	6.547e-5	0.33	10
p_c [Chan, 2-term]	9.754e-3	1.011e-5	6.545e-5	0.012	1e-4
p_c [Chan, 2-term upper bound]	9.754e-3	1.011e-5	6.545e-5	0.24	25
p_c [Coarse]	0.46	0.16	0.044	0.0062	0.010
Quadrature	9.7418e-3	1.0105e-5	6.5157e-5	0.0052374	0.0014893

or moves the avoidance regions of columns four and five closer to the origin, the coarse method will agree to within a few percent or better with quadrature. In such cases, Chan's method may produce error bounds that are on the order of $\pm 10^5$.

Table 2 illustrates a design trade for a simple case of the problem this paper addresses. In this example, two satellites are to form a "string of pearls" or in-track formation in a nearly circular orbit, with some nominal separation. When the mission flies, navigation and maneuver execution errors, as well as unmodeled perturbations, will preclude the satellites from reaching exactly the relative orbits that the mission planners desire, so that over time they will drift off station. Errors and perturbations that affect their relative semi-major axis will cause the fastest drift, which will be in the direction tangent to the orbits, i.e. the in-track direction. Gottlieb et al.[13] studied a similar problem, and showed that unless the semi-major axis errors of the orbit determination solutions for spacecraft in a low Earth orbit constellation are on the order of a few tens of meters or better, it may be safer not to maneuver for collision avoidance at all. In any case, during mission operations, accurate computation of collision probability is essential to avoid false alarms that would waste fuel, or missed detections that could jeopardize the mission. During the preliminary design phase however, conservative bounds on the collision probability are adequate for comparisons such as those in Table 2. From the table, it is easy to see the boundary at which one may trade between predictive navigation accuracy and nominal minimum approach distance, while keeping the collision probability small.

Even for more general formations, one may follow a procedure similar to that just described to get a rough sense of the trade between navigation accuracy, minimum approach distance, and collision probability, since errors in relative semi-major axis will be the largest source of relative drift, and hence the most significant contributor to the collision probability. For non-circular orbits, the relationship between in-track drift per revolution and semi-major axis error depends on where in the orbit one evaluates the relationship. In general, if one evaluates the drift at the true anomaly f_o every orbit, then

$$\sigma_{\Delta s}(f_o) = 3\pi \frac{1 + \epsilon \cos f_o}{\sqrt{1 - \epsilon^2}} \sigma_{\Delta a} \tag{27}$$

which will be a maximum at periapse and a minimum at apoapse. Tables 3 and 4 illustrate these bounds

Table 2. Coarse upper bound on probability of collision, as a function of predictive navigation accuracy, measured by relative semi-major axis standard deviation, $\sigma_{\Delta a}$, and nominal minimum approach distance, D, for an avoidance radius of 5 meters and a prediction interval of one orbit period of a circular orbit. The second column shows the one-sigma in-track error, $\sigma_{\Delta s}$, due to the semi-major axis error.

$p_c[\%]$		$D[\text{m}]$			
$\sigma_{\Delta a}[\text{m}]$	$\sigma_{\Delta s}[\text{m}]$	500	275	150	75
1	9.4	0.00	0.00	0.00	0.00
5	47	0.00	0.00	0.10	> 1
10	94	0.00	0.21	> 1	> 1
15	141	0.02	> 1	> 1	> 1
25	236	> 1	> 1	> 1	> 1

for the trade space of a highly elliptical orbit formation, with a much larger avoidance region.

Table 3. Coarse upper bound on probability of collision at apoapse, for an avoidance radius of 200 meters and a prediction interval of one orbit period, for $e = 0.8$.

$p_c[\%]$		$D[\text{m}]$			
$\sigma_{\Delta a}[\text{m}]$	$\sigma_{\Delta s}[\text{m}]$	2000	1100	600	300
5	16	0.00	0.00	0.00	0.00
25	79	0.00	0.00	0.00	> 1
50	160	0.00	0.00	0.54	> 1
75	240	0.00	0.01	> 1	> 1
125	390	0.00	> 1	> 1	> 1

Table 4. Coarse upper bound on probability of collision at periapse, for an avoidance radius of 200 meters and a prediction interval of one orbit period, for $e = 0.8$.

$p_c[\%]$		$D[\text{m}]$			
$\sigma_{\Delta a}[\text{m}]$	$\sigma_{\Delta s}[\text{m}]$	20000	11000	6000	3000
5	140	0.00	0.00	0.00	0.00
25	710	0.00	0.00	0.00	0.00
50	1400	0.00	0.00	0.00	> 1
75	2100	0.00	0.00	0.31	> 1
125	3530	0.00	0.11	> 1	> 1

An additional step one could consider is to compute the statistics of the time between collision avoidance maneuvers. Reference 14 describes a technique for determining the probability density of the time for the spacecraft to drift a specified relative distance, as a function of the ratio of D and $\sigma_{\Delta s}$. Based on the results above, one could specify a limit on the size of the relative "control box" in which the satellites must station-keep, to maintain the probability of collision within a given upper bound.

Although one could imagine a more refined set of analysis that incorporates nominal relative motion trajectories and the results of navigation system covariance analysis, for such an approach, the use of the coarse collision probability bound would not be justified. In the context of these more detailed analysis methods, quadrature, monte carlo analysis, and/or the use of any of the more accurate approximate methods available from the literature would better serve the analyst's purpose.

VI.   Summary

This work has proposed a coarse upper bound for estimating the collision probability between two spacecraft that is suitable for use in the preliminary design phase of satellite formations. It produces reasonable bounds

on the probability for cases which Chan's otherwise superior technique is not designed to cover. Because the bound can be highly conservative, it is not appropriate for operational scenarios or detailed design problems, as it could generate an excessive false alarm rate or overly conservative designs, respectively, under some conditions. However, it is a convenient and simple approach for rapidly examining the boundaries in the trade space of navigation accuracy, minimum nominal approach, and collision probability. It also provides a complementary analysis tool to the existing analytical method that Chan has developed.

VII.   Acknowledgments

References

[1] Foster, Jr., J. L. and Estes, H. S., "A Parametric Analysis of Orbital Debris Collision Probability and Maneuver Rate for Space Vehicles," Tech. Rep. JSC–25898, NASA Johnson Space Center, Houston, TX, 1992.

[2] Akella, M. R. and Alfriend, K. T., "Probability of Collision Between Space Objects," *Journal of Guidance, Control and Dynamics*, Vol. 23, No. 5, September–October 2000, pp. 769–772.

[3] Patera, R. P., "A General Method for Calculating Satellite Collision Probability," *Space Flight Mechanics 2000*, Univelt, San Diego, CA, 2000.

[4] Chan, K., "Improved Analytical Expressions for Computing Spacecraft Collision Probabilities," *Space Flight Mechanics 2003*, Univelt, 2003.

[5] Papoulis, A., *Probability, Random Variables, and Stochastic Processes*, chap. 7, McGraw-Hill, 2nd ed., 1965, pp. 194–196.

[6] Peterson, G. E., "Effect of Large Velocity Covariance on Collision Probability Computation," *Astrodynamics 2003*, Univelt, 2003.

[7] Chan, K., "Spacecraft Collision Probability for Long-Term Encounters," *Astrodynamics 2003*, Univelt, 2003.

[8] Chan, K., "Formation Flying: Collision Assessment, Pre-Emptive Maneuvers, and Safe-Haven Parking," *2003 Flight Mechanics Symposium*, NASA CP–2003–212246, 2003.

[9] Campbell, M. E., "Collision Monitoring and Avoidance in Satellite Clusters," *to appear in IEEE Transactions on Control System Technology*, 2004.

[10] Junkins, J. L., Akella, M. R., and Alfriend, K. T., "Non-Gaussian Error Propagation in Orbital Mechanics," *Journal of the Astronautical Sciences*, Vol. 44, No. 4, October–December 1996, pp. 541–563.

[11] Lee, D.-J. and Alfriend, K. T., "Effect of Atmospheric Density Uncertainty on Collision Probability," *Space Flight Mechanics 2000*, Univelt, 2000.

[12] Papoulis, A., *Probability, Random Variables, and Stochastic Processes*, McGraw-Hill, 3rd ed., 1984.

[13] Gottlieb, R. G., Sponaugle, S. J., and Gaylor, D. E., "Orbit Determination Accuracy Requirements for Collision Avoidance," *Space Flight Mechanics 2001*, Univelt, 2001.

[14] Carpenter, J. R. and Alfriend, K. T., "Navigation Accuracy Guidelines for Orbital Formation Flying," *Proceedings of the Guidance, Navigation, and Control Conference*, AIAA, Reston, VA, August 2003.